Annu. Rev. Nucl. Part. Sci. 1995. 45:133–61

CHARMED MESON SPECTROSCOPY

John Bartelt

Department of Physics and Astronomy, P.O. Box 1807, Station B, Vanderbilt University, Nashville, Tennessee 37235

Shekhar Shukla

Fermi National Accelerator Laboratory, P.O. Box 500, Batavia, Illinois 60510

CONTENTS

1. INTRODUCTION 134
2. THEORETICAL PREDICTIONS 137
3. EXPERIMENTAL OVERVIEW 140
   3.1 Experimental Difficulties 140
   3.2 Decay Characteristics of P-Wave Charmed Mesons 141
   3.3 Angular Distributions 142
4. DISCUSSION OF MEASUREMENTS 143
   4.1 Assignment of Spin and Parity to Observed States 144
   4.2 Masses and Widths 145
   4.3 Branching Ratios 149
   4.4 Angular Distributions 151
   4.5 Production Characteristics 153
5. COMPARISON OF EXPERIMENTAL RESULTS AND THEORETICAL PREDICTIONS 155
   5.1 Heavy-Quark Symmetry 155
   5.2 Quark Model 156
6. FUTURE MEASUREMENTS 158
   6.1 Future Measurements of Known Mesons 158
   6.2 Other Charmed Mesons Yet to be Observed 159
7. CONCLUSIONS 160

KEY WORDS: D^{**}, heavy quark, quark models, P-wave mesons, hadron spectroscopy

ABSTRACT

This article reviews experimental data on the orbitally excited charmed mesons, commonly called D^{**}s, including measurements of their masses and widths as

0163-8998/95/1201-0133$5.00

well as information on their production and decay properties. We use all available experimental data to calculate average values for the masses and widths of the six known D^{**+}s. Measurements of branching ratios, decay angular distributions, and production momentum spectra are tabulated. We also summarize the evidence supporting their spin-parity assignments. The measurements are compared with theoretical predictions from a quark model and from calculations using heavy-quark symmetry. Prospects for future measurements of these D^{**}s and of other excited states yet to be discovered are discussed.

1. INTRODUCTION

In the decade following the discovery of open charm (~1975–1984), six charmed mesons—three pseudoscalar and three vector states—were found and studied. The subsequent decade (~1985–1994) saw the discovery of six more charmed mesons (1). On the basis of the available data, we can confidently identify these states as P-wave ($L = 1$) mesons. In this article we review what has been learned about these new states.

The motivation for studying charmed mesons is twofold. First, if we know the properties of charmed mesons, we can test the assumptions in the various theoretical calculations and thus better understand the strong interaction. Second, this knowledge is useful in the study of B mesons because B mesons usually decay to charmed mesons. Moreover, because B mesons, like charmed mesons, are made up of one heavy quark and one light quark, a good understanding of the charmed mesons makes it possible to predict the properties of B mesons based on relatively simple theoretical calculations. This finding is especially important for the excited B mesons, for which experimental data to date are rather limited (see, for example, 2).

There has been much theoretical interest in systems such as D^{**}s that contain one heavy quark. This interest stems largely from the discovery of heavy-quark symmetry (HQS; see Section 2). Theorists have made detailed predictions about charmed and bottom hadrons using this symmetry. These predictions, as well as earlier predictions from quark models, should be tested in the charm sector. Discrepancies between theory and experiment can enable investigators to gauge the size of the corrections needed to account for the finite mass of the charmed quark. Such information will be necessary when these models are applied to the bottom sector. With the continuing interest in B meson physics, accurate theoretical models and predictions for systems with one heavy quark are important. These include the calculation of strong interaction parameters needed to interpret weak interaction effects, such as mixing and CP violation. Also, a complete understanding of the semileptonic decay of B mesons will require accurate measurements of $B \to D^{**}\ell\nu$ decays.

To help place the D^{**}s in context, we briefly review the pseudoscalar and vector charmed mesons. Since the discovery of the charmed pseudoscalar states, D^0, D^+, D_s^+, beginning in 1976 (3), a wealth of information has been accumulated on their properties. Because these are the lightest states carrying the charm quantum number, they decay via the weak interaction. They have lifetimes of the order of a picosecond. The corresponding vector states (D^{*0}, D^{*+} and D_s^{*+}) are also quite well known. They decay via the strong and electromagnetic interactions. For both the pseudoscalar and the vector states, the charged meson is a few MeV heavier than the neutral meson, and the strange meson is ~100 MeV heavier than the charged meson (see Table 1 for more details) (1). In each flavor doublet, the mass difference between the vector and pseudoscalar states is ~142 MeV, just a few MeV more than the mass of a pion. This mass splitting severely restricts the phase space available for strong decays and causes the vector states to be so narrow as to make the radiative decay significant. In the case of the D_s^{*+}, isospin conservation further suppresses the pionic decay, so that the radiative decay is dominant.

The first observation of an orbitally excited charmed meson was reported in 1986 by the ARGUS collaboration (4) (see Figure 1). As was initially suggested, this resonance was found to be a composite of two states (5). The experimental study of the D^{**}s began with this finding. In particular, three doublets of mesons (neutral, charged, and strange) have been observed that are believed to be states in which the quark-antiquark pair has one unit of orbital angular momentum. These doublets are ~450 MeV heavier than the vector states. Considerable theoretical work has also been done on the properties of these excited charmed mesons [6–8 and references therein].

In contrast to the narrow pseudoscalar D and vector D^* states, the D^{**}s have appreciable widths, resulting in a considerable increase of the background under the observed signals. Also, in each doublet, the two D^{**}s overlap, making accurate mass and width measurements more difficult (except in the case of the strange mesons). In addition, the production cross sections are typically an

Table 1 Masses and widths of the S-wave charmed mesons

Meson	Mass (MeV)	Γ
D^0	1864.6 ± 0.5	$2.41 \pm 0.02 \times 10^{12}$ s^{-1}
D^+	1869.4 ± 0.4	$0.95 \pm 0.01 \times 10^{12}$ s^{-1}
D_s^+	1968.5 ± 0.7	$2.14 \pm 0.08 \times 10^{12}$ s^{-1}
D^{*0}	2006.7 ± 0.5	<2.1 MeV, 90% c.l.
D^{*+}	2010.0 ± 0.5	<0.131 MeV, 90% c.l.
D_s^{*+}	2110.0 ± 1.9	<4.5 MeV, 90% c.l.

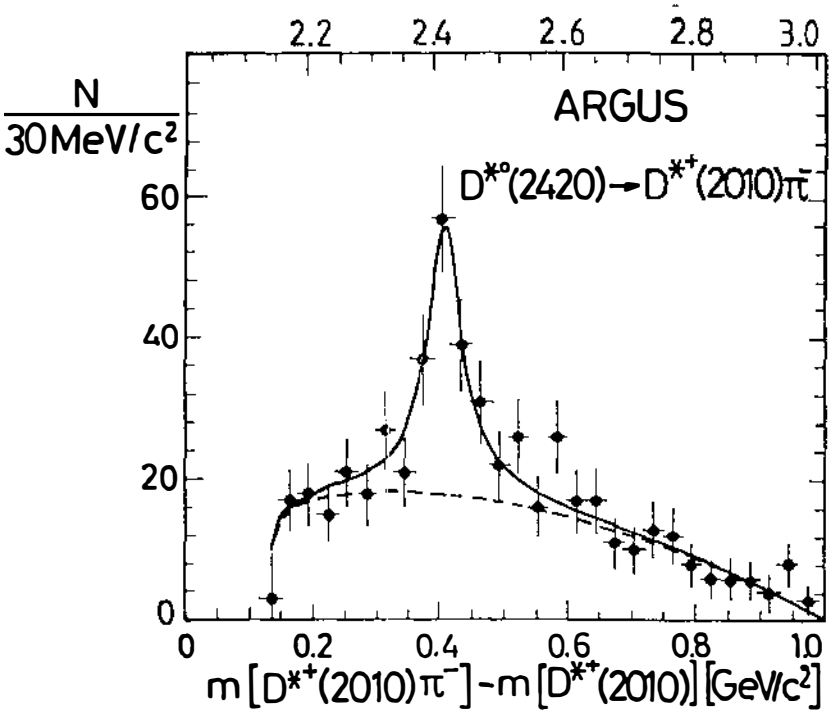

Figure 1 The $D^{*+}\pi^{-}$–D^{*+} mass difference spectrum from ARGUS showing the first observation of a $D^{**}(4)$. The solid line is a fit to the data.

order of magnitude smaller than those for the S-wave states, resulting in a reduction of the signal.

For mesons formed from equal-mass quarks, the total spin S is a good quantum number. This is true, for example, of quarkonium states ($c\bar{c}$ and $b\bar{b}$ mesons). S can have a value of 0 or 1; when combined with the orbital angular momentum (if $L > 0$), this yields a singlet and a triplet of states. For example, when $L = 1$, the singlet has quantum numbers $S = 0$, $J = 1$ and the triplet has quantum numbers $S = 1$ and $J = 0$, 1, or 2. This situation is analogous to LS coupling in atomic physics. Because $L = 1$, P-wave states have positive parity. The two $J = 1$ states, with $S = 0$ and 1, do not mix because they have opposite C parity.

In contrast, when one quark is heavy and the other light, S is no longer a good quantum number and the states do not have definite C parity. The observable $J = 1$ states are then mixtures of the $S = 0$ and $S = 1$ states. Examples of such mixing are the $K_1(1270)$ and $K_1(1400)$ mesons. In the limit $m_Q \to \infty$, the spin of the heavy quark decouples from the rest of the system. The observable

states can be labeled by the total angular momentum of the light quark j, which becomes a conserved quantity. For $L = 1$, we have states with $j = 1/2$ or 3/2. Combining j with the spin of the heavy quark produces two doublets: $j = 1/2$, $J = 0$ or 1 and $j = 3/2$, $J = 1$ or 2. This is analogous to JJ coupling. Again, the states have positive parity.

At present, there is no universally established notation to distinguish the two $J^P = 1^+$ states. We adopt the following notation, which has been used by several authors: $1^+_{1/2} \equiv (J^P = 1^+,\ j = 1/2)$, and $1^+_{3/2} \equiv (J^P = 1^+,\ j = 3/2)$ (see 6). When discussing the experimental results, however, we may drop the 3/2 subscript. The doublet memberships of the 0^+ and 2^+ states are not ambiguous, but they can be designated $0^+_{1/2}$ and $2^+_{3/2}$.

Conservation of angular momentum and parity requires that the 0^+ meson decay via an S wave (to 0^-0^- final states) and that the 2^+ meson decay via a D wave (to 0^-0^- or 1^-0^- states). The 1^+ states can decay via either an S wave or a D wave (only to 1^-0^- final states). However, HQS imposes a new restriction: In the limit of an infinitely heavy quark, the $1^+_{1/2}$ state must decay via an S wave, whereas the $1^+_{3/2}$ state must decay purely via a D wave. The $j = 3/2$ states are therefore expected to be relatively narrow ($\Gamma \sim 20$ MeV), whereas the $j = 1/2$ states are expected to be quite broad ($\Gamma \sim 200$ MeV or more). As we show below, predictions for the $j = 3/2$ mesons have been verified by experiment.

In this review, we give an overview of the theoretical models and predictions and a summary of the experimental situation, followed by a comprehensive review of the data on D^{**}s. Next, we compare the data with theoretical predictions. We conclude with a brief outlook on the future of charmed meson spectroscopy.

Throughout this article, reference to any charge state (particle or reaction) implies the inclusion of the charge conjugate state. Whenever two sets of errors are quoted for an experimental result, the first is the statistical and the second the systematic error.

2. THEORETICAL PREDICTIONS

In 1976, De Rújula et al (9) made the first prediction of the properties of the P-wave charmed mesons. They used a nonrelativistic quark model in which the short-range interquark interaction is described by a Coulomb-like potential. The authors described the four P-wave mesons in two doublets. Several other quark model calculations have been performed, e.g. by Schnitzer (10), by Pignon & Piketty (11), and more recently by Godfrey & Kokoski (7). Most of these authors used the sum of a Coulomb and a linear term to describe the interquark potential. The quark model calculations simplify considerably in

the limit of infinite mass for the heavy quark. In this limit, the spin-orbit interaction involving the spin of the heavy quark can be neglected. The mass spectrum is then determined by the total angular momentum of the light quark, $j = L + s_\ell$. The P-wave meson has two energy levels corresponding to $j = 1/2$ and $j = 3/2$. A doublet of degenerate states corresponds to the two values of the total angular momentum J of the meson, $J = j + s_c$. The finite mass of the heavy quark removes this degeneracy.

Some recent calculations do not use detailed quark model descriptions but are based on the heavy-quark effective theory (HQET). Isgur & Wise (12) showed that the strong interactions of systems with one heavy quark ($m_Q \gg \Lambda_{QCD} \approx$ 200 MeV) may be approximated by HQET, which is constructed from QCD in the limit when the mass of the heavy quark approaches infinity. In the limit of infinite quark mass, HQET exhibits a flavor-spin symmetry, i.e. the strong interaction properties of a meson containing a heavy quark do not depend on the flavor (mass) or spin of the heavy quark. This flavor and spin independence is called heavy-quark symmetry (HQS). Although not infinitely massive, systems containing one charmed quark do exhibit properties predicted by HQET.

This finding is particularly interesting since, in many cases, it is difficult to make accurate calculations using quantum chromodynamics (QCD), whereas quantitative predictions can be made by exploiting HQS. HQS can be used, for example, in calculating decay constants and form factors, which in turn help determine weak interaction parameters such as the Cabibbo-Kobayashi-Maskawa matrix elements (see 13 and 14 for recent reviews). Many recent theoretical predictions involving D^{**}s also use HQS. However, many predictions using the heavy-quark limit, including masses and partial widths, were made before Isgur & Wise discovered the explicit symmetry (see, for example, 6 and references therein).

Among the most detailed sets of recent D^{**} predictions are those by Godfrey & Kokoski (7) and by Eichten

mixing angle predictions for strange, charmed, and bottom mesons as well as partial width calculations for charmed and bottom mesons. The latter authors predict the masses and total widths of these states and of the D-wave, $j = 5/2$ strange, charmed, and bottom mesons.

Godfrey & Kokoski (7) use a quark potential model that includes one-gluon exchange and a linear confining potential. For decay rates they present calculations from two strong decay models: a pseudoscalar emission (PSE) model and a flux tube–breaking (FTB) model. They calculate the mixing angles that relate the physical $1^+_{1/2}$ and $1^+_{3/2}$ mesons to the singlet ($^1P_1$) and triplet ($^3P_1$) states:

$$1^+_{1/2} = -^1P_1 \sin\theta + {}^3P_1 \cos\theta$$

and

$$1^+_{3/2} = +^1P_1 \cos\theta + {}^3P_1 \sin\theta.$$

Their calculation yields $\theta = -26°$ for the nonstrange and $\theta = -38°$ for the strange charmed mesons.

Eichten et al (8) used HQS and data on excited K mesons and D^{**}s to predict the properties of the D_s^{**+}s and excited bottom mesons. Their most recent calculation of the $D_{s1}(2536)^+$ mass is low by ~10 MeV, which they take to be a "measure of the limitations" of their method. They predict the mass splitting between the D^+_{s1} and the D^{*+}_{s2} to be 35 MeV, which is in good agreement with the measured value of 38 MeV. Table 2 compares the mass and total width predictions for the charmed P-wave mesons (for additional predictions see Reference 6).

The partial and total width predictions are sensitive to the phase space available for the decays. This is particularly true for the charmed strange mesons, which are quite close to their strong decay thresholds. Thus, width predictions can be made more accurately by using the actual masses of the states than by using the theoretically predicted masses. Godfrey & Kokoski provide "reduced amplitudes," with the phase space factor removed, to facilitate such adjustments.

Because some of the theoretical uncertainties cancel in the ratios of widths (or partial widths), the ratios are probably more reliable than absolute width predictions. In HQS calculations, the predictions for mass splittings due to the finite mass of the heavy quark should be more accurate than the absolute masses.

One of the interesting predictions of the HQS-inspired models is that the narrow $1^+_{3/2}$ state should decay primarily via a D wave, even though an S wave is allowed, and might naively be expected to dominate. This result can be derived by treating j as a conserved quantum number (as it is in the limit $m_Q \to \infty$). Decoupling the heavy quark from the rest of the system allows us

Table 2 D^{**} mass and width predictions from Godfrey & Kokosi (G & K) (7) and Eichten, Hill & Quigg (EHQ) (8)[a]

Meson	G & K Mass (MeV)	EHQ Mass (MeV)	G & K Γ (MeV)	EHQ Γ (MeV)
$c\bar{u}\ 2^+$	2500	2459 (input)	37	28[a]
$c\bar{u}\ 1^+_{3/2}$	2460	2424 (input)	38	18
$c\bar{s}\ 2^+$	2590	2561	16	11
$c\bar{s}\ 1^+_{3/2}$	2550	2526	1.9	<1

[a]This total width was partially constrained to agree with data.

to treat the decay purely in terms of the degrees of freedom of the light quark. The decays of the $1^+_{1/2}$ and $1^+_{3/2}$ states (by emission of a single pseudoscalar) can then be seen as:

$$1/2^+ \rightarrow 1/2^- \, 0^-$$

and

$$3/2^+ \rightarrow 1/2^- \, 0^-,$$

respectively, where the first decay must proceed via an S wave and the second decay via a D wave because of conservation of angular momentum and parity.

By examining the decays of the $1^+_{3/2}$ D^{**}s to $D^*\pi$ and by measuring the helicity distribution of the daughter D^*s through their subsequent decays to $D\pi$, we can obtain experimental information on the relative strengths of the partial waves. The measured angular distibutions also have been used to help establish that the mesons under study are indeed 1^+ and 2^+ states.

For a finite-mass charmed quark, HQET does not make an explicit prediction for the relative sizes of the S and D waves. As Ming-Lu et al (15) pointed out, HQET predicts that the S-wave partial decay width of the $1^+_{3/2}$ should be small compared with typical S-wave decays. However, it may be comparable to (or larger than) the D-wave decay.

3. EXPERIMENTAL OVERVIEW

3.1 *Experimental Difficulties*

All six of the narrow $L = 1$ charmed mesons have been observed, but none of the broader $L = 1$ or higher excited states have been detected as of now. The excited states, which are more massive than their ground state counterparts, have smaller production cross sections, and efforts to measure these states have suffered from limited statistics. Other factors that complicate the experimental study of excited charmed mesons include: (*a*) larger combinatoric background, (*b*) peaks resulting from other states that overlap with or are close to the peak of interest, and (*c*) lower reconstruction efficiency. We briefly discuss these three factors.

3.1.1 COMBINATORIC BACKGROUND The higher combinatoric background results from the higher multiplicity of decay products and from the larger intrinsic widths of the states. In fixed-target experiments, there is an additional source that might dominate the other two contributions to the increased combinatoric background. This increase in background results from the lack of experimentally observable separation between the production and the decay verticies of the D^{**}s. In the case of a weakly decaying hadron, the

production and decay vertices are visibly separated; only tracks from a secondary vertex are used to construct candidates for the charm state. In the case of D^{**}, tracks from the D^{**} decay cannot be distinguished from tracks from fragmentation following charm production, thus increasing the number of combinations that must be included. Because the background increases with primary vertex multiplicity, it is expected to be worse in hadroproduction than in photoproduction.

3.1.2 OTHER STRUCTURES IN MASS DISTRIBUTIONS Determination of the background under the peak requires a region of smoothly varying background below and/or above the peak. In a mass distribution, other structures in the same mass region can make it difficult to estimate the background shape under a peak resulting from a D^{**}. These structures may result from the same state in a partially reconstructed decay mode or from other states that have been either partially or fully reconstructed. For example, the two peaks in the $D^{*+}\pi^-$ mass distribution arise from the decay of the two members of $j = 3/2$ doublet (see Section 4.2.3). When the ARGUS collaboration (4) first observed this signal resulting from an excited charm state, it was unclear whether the signal represented one or more resonances. We now know that the broad peak is actually composed of two overlapping $2^+_{3/2}$ and $1^+_{3/2}$ states.

3.1.3 RECONSTRUCTION EFFICIENCY The excited states generally have a lower reconstruction efficiency than the ground states partly because they have higher multiplicity decays and more tracks and/or photons must be successfully reconstructed. For the current fixed-target experiments, this problem is compounded somewhat because they were designed without much attention to the acceptance for these states.

3.2 *Decay Characteristics of P-Wave Charmed Mesons*

The $L = 1$ charmed mesons are expected to decay strongly, mostly through two-body decays. The allowed two-body decays are listed in Table 3. Other two-body decays are prohibited because of conservation of angular momentum

Table 3 Allowed two-body strong decays of the P-wave charmed mesons

j	J^P	D^{**} decay modes	D_s^{**+} decay modes
3/2	2^+	$D\pi, D^*\pi, D\rho, D^*\rho$	DK, D^*K
3/2	1^+	$D^*\pi, D\rho, D^*\rho$	D^*K
1/2	1^+	$D^*\pi, D\rho, D^*\rho$	D^*K
1/2	0^+	$D\pi, D^*\rho$	DK

and parity. Strong decays of the D_s^{**+} to $D_s^+\pi^0$ or to $D_s^{*+}\pi^0$ are forbidden by conservation of isospin; decays to $D_s^+\pi\pi$ are suppressed by the Okuba-Zweig-Iizuka rule. The D^{**}s are only ~450 MeV more massive than the D^*s; thus the decays to $D\rho$ and to $D^*\rho$ are possible only because of the large width of the ρ.

The $J = 2$ state can decay to $D\pi$ or to $D^*\pi$. Both are D-wave decays; thus the state should be fairly narrow. The $J = 0$ state can decay to $D\pi$ but not to $D^*\pi$. The decay proceeds via an S wave, and the state is expected to be broad, i.e. a width of several hundreds of MeV, according to Godfrey & Kokoski (7). The $J = 1$ states can decay to $D^*\pi$ but not $D\pi$. The relative angular momentum of the decay products can be either 0 or 2 (see Section 2). However, the $1^+_{3/2}$ state is expected to decay predominantly via a D wave and to be narrow, whereas the $1^+_{1/2}$ state is expected to decay predominantly via an S wave and to be broad [several hundred MeV (7)]. The similarity of the doublet partners becomes apparent: The 2^+ and $1^+_{3/2}$ decay via a D wave and are narrow, whereas the 0^+ and $1^+_{1/2}$ decay via an S wave and are broad.

3.3 *Angular Distributions*

For the 2^+ decay to 1^-0^- (e.g. to $D^{*+}\pi^-$), the decay must proceed via a D wave. This forces the vector meson (D^{*+} in this example) to assume a helicity of ± 1. When the vector state decays to two pseudoscalars (e.g. $D^{*+} \rightarrow D^0\pi^+$), the angular distribution will reflect this helicity. The helicity angle α is defined as the angle between the π^- (i.e. the pseudoscalar from the first decay) and the π^+ (i.e. one of the pseudoscalars from the second decay), measured in the rest frame of the D^{*+}(i.e. the vector). This decay chain produces a helicity angle distribution proportional to $\sin^2\alpha$. Such a distribution proves that the parent state must have "natural" spin parity (i.e. 1^-, 2^+, 3^-, etc). This angular distribution is independent of the alignment of the parent state; however, care must be taken that the efficiency of detection does not depend on the decay angle (θ) of the initial state. The decay angle is defined as the angle between the D^{**} in the lab frame and the π^- in the the D^{**} rest frame. If the acceptance is not uniform in the decay angle, the helicity angle distribution can be distorted (see Equation 1, below).

On the other hand, the decay of a 1^+ (an "unnatural" spin parity) will have a helicity angle distribution that is flat if the decay is a pure S wave or that is proportional to $1 + 3\cos^2\alpha$ if the decay is a pure D wave. The same is true for other unnatural spin parities (2^-, 3^+, 4^-, etc), except for 0^-, which must have a $\cos^2\alpha$ distribution. See Table 4 for a summary of the helicity distributions.

Table 4 Helicity angle distributions for the decay to 1^-0^- final states of various types of parent mesons

Spin-parity of the parent meson	Helicity angle distribution
0^+	decay forbidden
0^-	$\propto \cos^2\alpha$
$1^-, 2^+, 3^- \ldots$	$\propto \sin^2\alpha$
$1^+, 2^-, 3^+ \ldots$ S wave	constant
$1^+, 2^-, 3^+ \ldots$ D wave	$\propto 1 + 3\cos^2\alpha$

If both an S wave and a D wave are present, one must take into account a possible phase difference between them. The general form of the angular distribution is then (16):

$$\frac{dN}{(d\cos\alpha)(d\cos\theta)} \propto \frac{\sin^2\alpha}{8}\left[(1+\cos^2\theta)+\rho_{00}(1-3\cos^2\theta)\right]$$
$$\times\left[2\Gamma_S+\Gamma_D+2\sqrt{2\Gamma_S\Gamma_D}\cos\varphi\right]$$
$$+\frac{\cos^2\alpha}{2}\left[(1-\cos^2\theta)-\rho_{00}(1-3\cos^2\theta)\right]$$
$$\times\left[\Gamma_S+2\Gamma_D-2\sqrt{2\Gamma_S\Gamma_D}\cos\varphi\right], \quad 1.$$

where Γ_S and Γ_D are the partial wave widths, φ is the relative phase of the two amplitudes, and ρ_{00} is the fraction of the parent state with helicity 0 in the lab frame. Integrating over $\cos\theta$ from -1 to $+1$ (or from 0 to $+1$) and normalizing the results gives:

$$\frac{1}{N}\frac{dN}{d\cos\alpha} = \frac{1}{2}\left[R+(1-R)\left(\frac{1+3\cos^2\alpha}{2}\right)\right.$$
$$\left.+\sqrt{2R(1-R)}(\cos\varphi)(1-3\cos^2\alpha)\right], \quad 2.$$

where $R = \Gamma_S/(\Gamma_S + \Gamma_D)$. Again, this result is valid if the acceptance is uniform in the decay angle θ. Data can be fit with this form to find combinations of R and φ that are consistent with the data.

4. DISCUSSION OF MEASUREMENTS

Excited charmed (nonstrange) mesons have been observed at masses of ~2420 and ~2460 MeV and identified as $L = 1$ states with $J = 1$ and $J = 2$, respectively. The corresponding charmed strange states also have been observed

and are ~115 MeV heavier than the nonstrange states. The Particle Data Group refers to the $J = 2$ members as D_2^{*0}, D_2^{*+}, and D_{s2}^{*+} for the light-quark flavors u, d, and s, respectively (1). The corresponding $J = 1$ states are named D_1^0, D_1^+, and D_{s1}^+.

4.1 *Assignment of Spin and Parity to Observed States*

Although none of the spin parity assignments for the observed states has been rigorously proven, the circumstantial evidence in favor of the standard assignments is substantial and not subject to any serious challenge. We discuss this evidence below.

4.1.1 THE $J^P = 2^+$ STATES: D_2^{*0}, D_2^{*+}, AND D_{s2}^{*+} The $D_2^*(2460)^0$ has been observed to decay to $D^+\pi^-$ (16–20), whereas its isospin partner, $D_2^*(2460)^+$, has been seen in the $D^0\pi^+$ mass spectrum (19–22). The reasoning leading to the $L = 1$, $J = 2$ assignment for the D_2^{*0} is as follows: The lowest excited states that can decay to $D^+\pi^-$ are the $L = 1$ states with $J = 0$ and $J = 2$. These states are expected to be separated in mass by ~100 MeV (7). The $J = 0$ state is expected to be several hundreds of MeV wide, whereas the $J = 2$ state is expected to be narrow (a few tens of MeV) (7). The mass and width of the observed state are consistent with the predictions for the $J = 2$ state and inconsistent with those for the $J = 0$ state. The higher excited states ($L > 1$ or radial excitations) are expected to be $\gtrsim 300$ MeV heavier than the observed state (8).

If the observed state is indeed a $J^P = 2^+$ state, it should also decay to $D^{*+}\pi^-$. A significant shoulder is observed in the $D^{*+}\pi^-$ mass spectrum on the high side of a peak resulting from another state, the D_1^0. This shoulder is consistent with the decay of the D_2^{*0} to $D^{*+}\pi^-$. Additional evidence for the assignment of the spin-parity quantum numbers comes from the angular distribution of the $D^{*+}\pi^-$ (see Section 4.4), which is also consistent with the expectations of a $J^P = 2^+$ state. This observation does not, however, rule out other "natural" spin parity assignments.

Taken together, the data indicate that the D_2^{*0} is the lowest $L = 1$, $J = 2$ charmed state. Similar findings led to the same assignment of $L = 1$, $J = 2$ for the D_2^{*+}.

The $D_{s2}^{*+}(2573)$ recently was observed to decay to D^0K^+ (23). Again, the possible spin assignments for the D_{s2}^{*+} are $J = 0$ and $J = 2$. The narrow width supports a $J = 2$ assignment, which implies that the decay to D^*K should also occur, although it has not yet been observed. Because the decay to D^*K is expected to be highly suppressed owing to the limited phase space available, it does not conflict with the $J = 2$ spin assignment. Given the overall pattern of masses, widths, and decays of the six observed D^{**}s, this assignment seems quite likely.

4.1.2 THE $J^P = 1^+$ STATES: D_1^0, D_1^+, AND D_{s1}^+ The $D_1(2420)^0$ has been observed to decay to $D^{*+}\pi^-$ (5, 16, 19, 20). Apart from the D_2^{*0}, the only low-lying excited states that can decay to $D^{*+}\pi^-$ are the two $L = 1$, $J = 1$ states. The fact that the decay of $D_1(2420)^0$ to $D\pi$ has been searched for and not seen is in agreement with this assignment. The small width of the state, together with information on the angular distribution of its decay (see below), supports its assignment to the $j = 3/2$ doublet. The D_1^+ state recently observed (22) in the decay to $D^{*0}\pi^+$ has been identified as the isospin partner of the D_1^0 on the basis of its similar mass, width, and decay angular distribution. Thus, it is also believed to be a $1^+_{3/2}$ state.

The $D_{s1}(2536)^+$ has been observed to decay to D^*K but not to DK (19, 24, 25). This finding again indicates an assignment of $L = 1$ and $J = 1$. The extreme narrowness of the $D_{s1}(2536)^+$ indicates that it is a member of the $j = 3/2$ doublet.

4.2 *Masses and Widths*

The masses and widths of the D^{**}s have been determined by reconstructing their decays to $D^{[*]}\pi$ or $D^{[*]}K$ and calculating the mass difference between the D^{**} candidate and the D or D^*. Many of the measurement errors cancel in the difference, resulting in a substantial improvement in resolution. The D^{**}s appear as peaks in the mass difference spectrum, and the central values and widths can be extracted. We discuss these measurements below.

4.2.1 D_2^{*+} AND D_2^{*0} Figures 2 and 3 show mass difference distributions for $\Delta M = M(D^0\pi^+) - M(D^0)$ from experiments at Femilab E687 (19) and CLEO (22). The peak near $\Delta M \approx 600$ MeV is due to the D_2^{*+}. No other state of similar mass can decay to $D^0\pi^+$ (see Section 4.1.1). The $J^P = 0^+$ state should be 100 MeV lighter and very broad and thus cannot be confused with this state.

Unfortunately, the mass difference spectrum is complicated by structures resulting from partially reconstructed states on the low-mass side of the D_2^{*+} peak. These structures hamper accurate background determination. The enhancement at $\Delta M \approx 450$ MeV is due to decays of both the D_2^{*+} and the D_1^+ to $D^{*0}\pi^+$, with the D^{*0} decaying to $D^0\pi^0$. The π^0 has not been reconstructed, but because the Q-value for the D^{*0} decay is small, the effective mass distribution for the partially reconstructed decay results in a relatively narrow enhancement that is shifted in mass by about one pion mass. Because the interval between this satellite peak and the D_2^{*+} peak is not large enough to reliably determine the background, it is necessary to use the mass range beyond this structure.

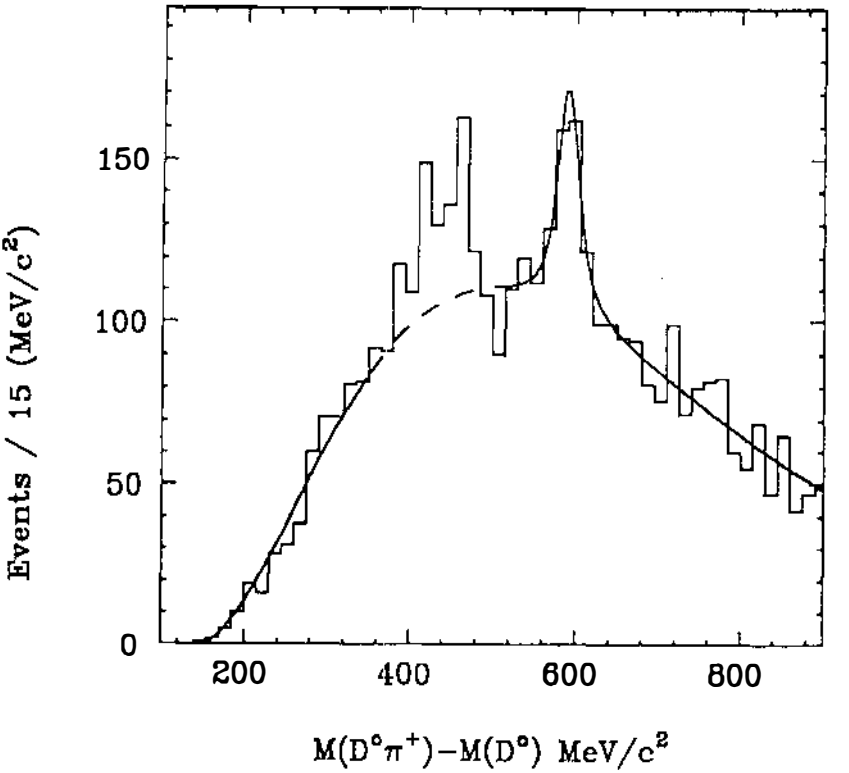

Figure 2 The $D^0\pi^+$–D^0 mass difference spectrum from Fermilab experiment E687 showing the D_2^{*+} (peak included in the fit) and other structures (19). The solid line is a fit to the data. The lower peak is from other, partially reconstructed, D^{**} states, primarily from events with a D_1^+. This enhancement is difficult to model and has been excluded from the fit.

However, other structures may prevent extension of the mass range on the low-mass side. Sources that could lead to such structures include the decays of the D_1^+ to $D^0\rho^+$ and of the D_1^0 to $D^0\rho^0$. Partial reconstruction of such decays using the D^0 and one of the pions from the ρ decay can produce a broad enhancement at lower masses. The size of such an enhancement in the observed mass distribution depends on the momentum spectrum of the charm production and on the acceptance of the apparatus.

Study of the D_2^{*0} using the $D^+\pi^-$ mass spectrum involves problems similar to those discussed above for the D_2^{*+}. Table 5 lists the experimental results on the masses and widths of the $J = 2$ (nonstrange) states. The problems in fitting the background are probably responsible for the large spread in the measured masses.

4.2.2 D_1^0 AND D_1^+ The $1^+_{3/2}$ state, D_1^0, has been observed to decay to $D^{*+}\pi^-$. The 2^+ state (D_2^{*0}) and the $1^+_{1/2}$ state can also decay to $D^{*+}\pi^-$. The $1^+_{1/2}$ state should be very wide and indistinguishable from the combinatoric background. However, the two $j = 3/2$ states are very close in mass and have comparable widths, making them difficult to resolve. An examination of the $D^{*+}\pi^-$ mass spectrum shows a broad structure at a mass of ~2420 MeV. We expect this structure to have contributions from both members of the $j = 3/2$ doublet. The 2^+ state can only decay via a D wave; according to the HQET, the $1^+_{3/2}$ state also should decay predominantly via a D wave.

As explained above, the decays of the secondary D^*s exhibit different helicity angle distributions. This difference can be used to separate the two states. A cut requiring $|\cos\alpha| > 0.8$, for example, virtually eliminates the 2^+ states while

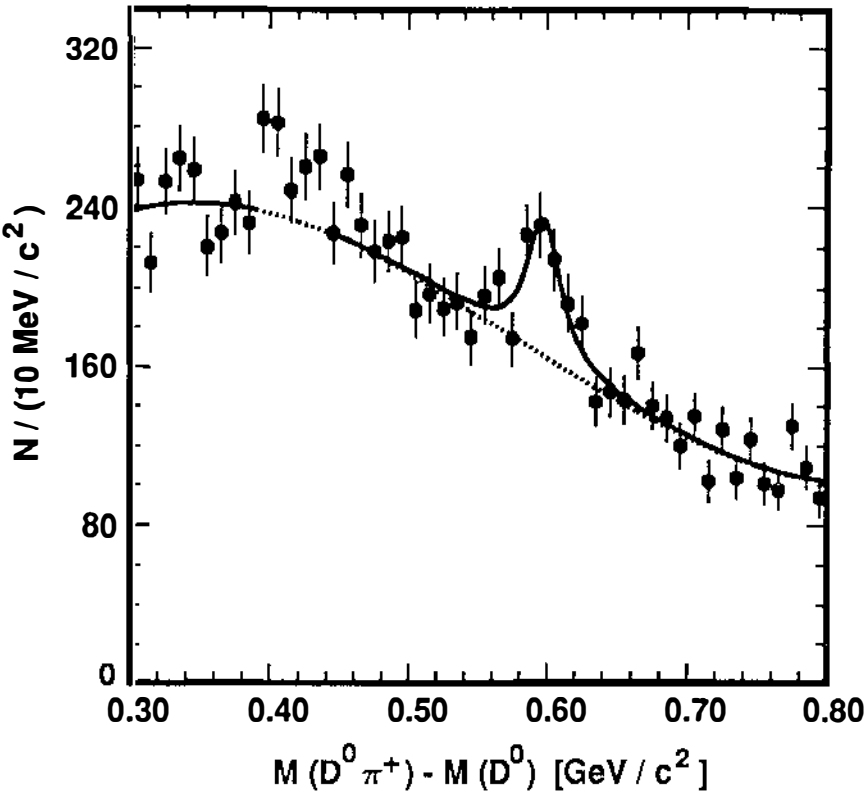

Figure 3 The $D^0\pi^+$–D^0 mass difference spectrum from CLEO showing the D_2^{*+} (peak included in the fit) and other structures (22). The solid line is a fit to the data.

Table 5 Mass and width measurements of the D_2^{*0} and D_2^{*+} mesons[a]

	D_2^{*0} $D_2^{*0} \to D^+\pi^-$		D_2^{*+} $D_2^{*+} \to D^0\pi^+$	
Experiment	Mass	Width	Mass	Width
ARGUS (18, 21)	$2455 \pm 3 \pm 5$	15^{+13+5}_{-10-10}	$2469 \pm 4 \pm 6$	27 ± 12
CLEO 1.5 (20)	$2461 \pm 3 \pm 1$	20^{+9+9}_{-12-10}		
CLEO II (16, 22)	$2465 \pm 3 \pm 3$	28^{+8+6}_{-7-6}	$2463 \pm 3 \pm 3$	$27^{+11}_{-8} \pm 5$
E687 (19)	$2453 \pm 3 \pm 2$	$25 \pm 10 \pm 5$	$2453 \pm 3 \pm 2$	$23 \pm 9 \pm 5$
E691 (17)	$2459 \pm 3 \pm 2$	$20 \pm 10 \pm 5$		
Average	2458.9 ± 2.0[a]	23 ± 5	2459.1 ± 4.2[b]	25^{+7}_{-6}

[a]Because of the disparity in the measurements, the error has been scaled up by a factor of 1.2 using the method of the Particle Data Group (1).
[b]Because of the disparity in the measurements, the error has been scaled up by a factor of 1.7 using the method of the Particle Data Group (1).

preserving a large part of the contribution from the $1^+_{3/2}$ state, thus enabling measurement of the mass and width of the latter. The isospin partner of the D_1^0, the D_1^+, is measured in a similar fashion. Results of measurements of the masses and widths are listed in Table 6. The recent measurements by CLEO and E687 are in good agreement.

4.2.3 D_{s1}^+ AND D_{s2}^{*+} The D_s^{**+}s do not suffer from the same problems as the nonstrange states, primarily because the strange states are very close to the edge of phase space. This proximity causes the $1^+_{3/2}$ state (D_{s1}^+) to be extremely narrow and the decay of the 2^+ state (D_{s2}^{*+}) to D^*K to be highly suppressed relative

Table 6 Mass and width measurements of the D_1^0 and D_1^+ mesons[a]

	D_1^0 $D_1^0 \to D^{*+}\pi^-$		D_1^+ $D_1^+ \to D^{*0}\pi^+$	
Experiment	Mass	Width	Mass	Width
ARGUS (5)	$2414 \pm 2 \pm 5$	$13 \pm 6^{+10}_{-15}$		
CLEO 1.5 (20)	$2428 \pm 3 \pm 2$	23^{+8+10}_{-6-4}		
CLEO II (16, 22)	$2421^{+1}_{-2} \pm 2$	20^{+6+3}_{-5-3}	$2425 \pm 2 \pm 2$	$26^{+8}_{-4} \pm 4$
E687 (19)	$2422 \pm 2 \pm 2$	$15 \pm 8 \pm 4$		
Average	2422.2 ± 2.2[a]	18^{+5}_{-4}		

[a]Because of the disparity in the measurements, the error has been scaled up by a factor of 1.3 using the method of the Particle Data Group (1).

Table 7 Mass and width measurements of the D_{s1}^+ meson

Experiment	Decay mode used	Mass	Width limit (90% CL)
ARGUS (5)	$D^{*+}K^0$	$2535.9 \pm 0.6 \pm 2.0$	<4.6
ARGUS (5)	$D^{*0}K^+$	$2535.2 \pm 0.5 \pm 1.5$	<3.9
CLEO 1.5 (20)	$D^{*+}K^0$	$2536.6 \pm 0.7 \pm 0.6$	<5.4
CLEO II (25)	$D^{*+}K^0$	$2534.8 \pm 0.6 \pm 0.6$	
CLEO II (25)	$D^{*0}K^+$	$2535.3 \pm 0.2 \pm 0.5$	<2.3
E687 (19)	$D^{*+}K^0$ & $D^{*0}K^+$	$2535.0 \pm 0.6 \pm 1.0$	<3.2
BEBC (28)	$D^{*+}K^0$ & $D^{*0}K^+$	2534.2 ± 1.2	
Average		2535.30 ± 0.53	<2.3

to DK. Thus the DK spectrum exhibits no significant satellite peak from partially reconstructed D_{s2}^{*+}s, and the satellite peak from partially reconstructed D_{s1}^+s is very narrow and easy to identify. The only significant background structure that might be problematic results from $D_2^{*+} \rightarrow D^0\pi^+$ decays that are misidentified as D^0K^+, but this is a minor problem (23). The results of measurements of the D_{s1}^+ are listed in Table 7. There is excellent agreement on the mass of the D_{s1}^+. In the experiments, the state was found to be very narrow, and only upper limits have been set on its width.

There is one systematic error on the D_{s1}^+ mass that is common to all of these measurements: the error on the D^0 mass. This error is the dominant uncertainty for the more accurate measurements. To derive the combined error of all measurements, we first subtracted this common error in quadrature from the error of each experiment, formed the average, and added the common error in quadrature to the error on the average. For this reason, our average differs slightly from the value cited by the Particle Data Group (1).

To date, only the CLEO collaboration has observed the D_{s2}^{*+} (23) at a mass of $2573.2^{+1.7}_{-1.6} \pm 0.9$ and with a width of $16^{+5}_{-4} \pm 3$. It is amusing to note that in 1986, when the Particle Data Group introduced their new naming convention for hadrons, they realized that it would "lead to some cumbersome symbols, such as a D_{s2}^{*+}," but they noted that "such particles are unlikely to be often seen." (26)

4.3 *Branching Ratios*

To date, few of the D^{**} branching ratios have been measured, simply because many of these states have been observed in only one decay mode. For the D_2^{*0} and the D_2^{*+}, both $D^*\pi$ and $D\pi$ modes have been measured, so we can present the ratios of these decay modes. For the D_{s1}^+

decay rates to $D^{*+}K^0$ and $D^{*0}K^+$. Other measurements set limits on decay modes that are forbidden or suppressed.

For the D_2^{*0}, the average ratio of the ARGUS (5), CLEO (20), and CLEO II (16) measurements is:

$$\frac{\mathcal{B}\left[D_2^{*0} \to D^+\pi^-\right]}{\mathcal{B}\left[D_2^{*0} \to D^{*+}\pi^-\right]} = 2.3 \pm 0.6,$$

where we have corrected the individual measurements for recent changes in the D^{*+} and D^+ branching fractions. The CLEO II collaboration (22) has measured the branching ratio

$$\frac{\mathcal{B}\left[D_2^{*+} \to D^0\pi^+\right]}{\mathcal{B}\left[D_2^{*+} \to D^{*0}\pi^+\right]} = 1.9 \pm 1.1.$$

These results are in good agreement with predictions, which range from 1.5 to 2.4 (6, 7). For the strange 2^+ state, CLEO II has set an upper limit (23):

$$\frac{\mathcal{B}\left[D_{s2}^{*+} \to D^{*0}K^+\right]}{\mathcal{B}\left[D_{s2}^{*+} \to D^0K^+\right]} < 0.33,$$

at 90% confidence level (c.l.). This ratio is predicted to be ~0.15 (7). (We have adjusted this prediction for phase space using the measured masses instead of the predicted masses.)

The CLEO II collaboration has also measured the ratio

$$\frac{\mathcal{B}\left[D_{s1}^{+} \to D^{*0}K^+\right]}{\mathcal{B}\left[D_{s1}^{+} \to D^{*+}K^0\right]} = 1.1 \pm 0.3.$$

The ARGUS group (27) has not explicity published this ratio but did provide sufficient information to allow us to derive their measurement of the same ratio, 1.4 ± 0.6. We have added all errors in quadrature, which is an overestimate because some systematic errors must cancel in the ratio. From isospin symmetry one would expect the ratio to be unity; however, the phase space available is different for the two decays. Assuming the decay is an S-wave decay, the phase space ratio is 1.13; alternatively, for a purely D-wave decay, the phase space ratio is 1.8. These ratios seem to rule out a dominant D-wave decay. This apparent contradiction with the HQET prediction can be resolved (see below).

In addition, CLEO 1.5 set an upper limit on the decay of the D_1^0 to $D^+\pi^-$ (20); this decay is forbidden for a meson with spin parity 1^+ or with any other unnatural spin parity. The limit, at 90% c.l., is

$$\frac{\mathcal{B}\left[D_1^0 \to D^+\pi^-\right]}{\mathcal{B}\left[D_1^0 \to D^{*+}\pi^-\right]} < 0.24.$$

Similarly, CLEO II set limits at 90% c.l. (22, 25):

$$\frac{\mathcal{B}\left[D_1^+ \to D^+\pi^0\right]}{\mathcal{B}\left[D_1^+ \to D^{*+}\pi^0\right]} < 0.18 \quad \frac{\mathcal{B}\left[D_{s1}^+ \to D^0 K^+\right]}{\mathcal{B}\left[D_{s1}^+ \to D^{*0}K^+\right]} < 0.12$$

and

$$\frac{\mathcal{B}\left[D_{s1}^+ \to D^+ K^0\right]}{\mathcal{B}\left[D_{s1}^+ \to D^{*+}K^0\right]} < 0.40$$

(22, 25). These ratios are all expected to be zero. ARGUS has set a limit on the last of these ratios, also at 90% c.l., of <0.43 (24).

CLEO II set a limit on the radiative decay of the $D_{s1}(2536)^+$:

$$\frac{\mathcal{B}\left[D_{s1}^+ \to D_s^{*+}\gamma\right]}{\mathcal{B}\left[D_{s1}^+ \to D^{*0}K^+\right]} < 0.42,$$

at 90% c.l. (25). This limit seems to contradict the observation by Asratyan et al (29), of a charmed strange resonance near 2535 MeV decaying to $D_s^{*+}\gamma$ but not to D^*K. Asratyan et al used a partial reconstruction technique, a method they later abandoned because of systematic problems (30).

4.4 *Angular Distributions*

As stated above (see section 3.3), by measuring in D^{**} decays the helicity of daughter D^*s from the analyses of the decay distributions we can learn something about the spin and parity of the parent D^{**} and about the relative strengths of the partial waves of the $1^+_{3/2}$ decays.

To measure the helicity angle distributions, experimenters must extract the number of events in a mass spectrum as a function of the helicity angle. In most cases, except for the D_{s1}^+, there are two overlapping resonances in the mass spectrum with presumably different angular distributions. Mismeasurement of the widths of the resonances will produce errors in the measurement of the angular distributions. This problem must be taken into account when estimating the systematic errors.

The ARGUS, E687, and CLEO II collaborations have studied the helicity angle distributions of the D^{**} states (5, 16, 19, 22, 25). These groups have tested specific hypotheses and have fit the data with the form $dN/d\cos\alpha \propto 1 + R\cos^2\alpha$. The fitted values of R are listed in Table 8. The ARGUS and CLEO collaborations found that the D_2^{*0} and D_2^{*+} data favor a helicity angle distribution proportional to $\sin^2\alpha$, as would be expected for 2^+ meson (5, 16, 22). However, the data are also consistent with a flat distribution.

For the D_1^0 and D_1^+, all of the measurements are consistent with a $1 + 3\cos^2\alpha$ distribution (e.g. a pure D-wave decay); the probability for other plausible

Table 8 Best fits to $dN/d\cos\alpha \propto (1 + R\cos^2\alpha)$ for helicity angle distributions[a]

Meson	Experiment	Fit value of R	χ^2/N_{dof}	c.l.
D_2^{*0}	ARGUS (5)	-0.4 ± 0.7	—	—
D_2^{*0}	CLEO (16)	$-0.74^{+0.49}_{-0.38}$	0.6/3	91%
D_2^{*+}	CLEO (22)	$-1.00^{+0.23}_{-0.00}$	1.3/2	51%
D_1^0	ARGUS (5)	2.8 ± 1.7	0.9/2	64%
D_1^0	CLEO (16)	$2.74^{+1.40}_{-0.93}$	2.2/3	53%
D_1^+	CLEO (22)	$3.55^{+5.26}_{-2.02}$	1.6/3	45%
D_{s1}^+	CLEO (25)	$-0.23^{+0.40}_{-0.32}$	—	—

[a]The value of R was constrained to lie between -1 and ∞ for this fit.

distributions is much lower (5, 16, 19, 22). On the other hand, the CLEO measurement of the $D_{s1}(2536)^+$ is consistent with a flat distribution (e.g. a pure S-wave decay) (25). This apparent contradiction with the HQET prediction for the D_{s1}^+ can be resolved by considering the phase space available for the decay to $D^{*0}K^+$. This decay is only 35 MeV above threshold; the decay products have a momentum of only 169 MeV/c in the D_{s1}^+ rest frame. [$D_{s1}(2536)^+ \rightarrow D^{*+}K^0$ is even closer to threshold.] This low momentum severely restricts a D-wave decay, for which the phase space is proportional to p^5 (here, p refers to the center-of-mass momentum of the daughter particles). In contrast, typical S-wave widths are of order of p. The total width of the D_{s1}^+ is <2.3 MeV; thus the S-wave amplitude clearly is highly suppressed by HQS (compare this, for example, to the decay $a_1 \rightarrow \rho\pi$). This result is in agreement with the HQET prediction and with that of Godfrey & Kokoski (7). The data are consistent with the S wave being the larger partial wave, as was also predicted by Godfrey & Kokoski (7). If the $D_{s1}(2536)^+$ were just a few dozen MeV heavier, the D wave would be the dominant partial wave.

For the D_1^0 and D_1^+, the CLEO II collaboration (16, 22) has also conducted a two-dimensional examination of the R and φ plane (see Section 3.3, Equation 2), where R is the fraction of the decay proceeding through the S wave and φ is the phase difference between the partial waves. They excluded some values of R and φ at 90% c.l. The analysis indicates that if $\varphi = 0$ ($\cos\varphi = 1$), then R is small ($\lesssim 5\%$). For larger values of φ, much larger values of R are allowed.

If the D^{**}s are produced with nonzero alignment, that is, with their spin axes having a preferred orientation, and if larger data samples are accumulated, it may be possible to measure R and φ separately (R Kutschke, private communication). Such a measurement would provide a definitive determination of the partial wave strengths.

4.5 *Production Characteristics*

One striking fact has been discerned about the production of D^{**}s in e^+e^- annihilation: Their momentum spectrum is significantly harder than that of the S-wave charmed mesons. This feature has been studied by the ARGUS and CLEO collaborations at center-of-mass energies of ~10.6 GeV (5, 16, 18, 22, 24, 25). If we only look at continuum production of charm (i.e. excluding B decay products), we see that the data generally have been fit with the Peterson fragmentation function (31):

$$\frac{dN}{dx} \propto \frac{1}{x[1-(1/x)-\epsilon_P/(1-x)]^2},$$

where x is p/p_{max}, the scaled momentum, and ϵ_P is the only adjustable parameter. Fits to the ARGUS and CLEO data give $\epsilon_P(D^0) = 0.135 \pm 0.010$ and $\epsilon_P(D^{*+}) = 0.078 \pm 0.008$ (1). These correspond to dN/dx peaking near $x = 0.6$ and $x = 0.7$, respectively. In contrast, the CLEO II collaboration has measured $\epsilon_P \sim 0.02$ for five of the D^{**}s, which corresponds to dN/dx peaking sharply near $x \approx 0.85$–0.9. The ARGUS group also has fit their data with the Peterson function and found somewhat larger values of ϵ_P, although still smaller than those of the S-wave charmed mesons. With the larger errors of the ARGUS data, the discrepancy between the CLEO and ARGUS measurements is only about two standard deviations for the D_1^0 and $D_{s1}(2536)^+$and about one standard deviation for the D_2^{*0}. The measurements are listed in Table 9.

The Peterson fragmentation function has been used to extrapolate the production cross section to $x = 0$; all measurements are done with minimum x cuts of ≥ 0.5. The cross section times the branching fraction measurements are listed in Table 10. There is also some disagreement between the measurements

Table 9 Measurements of Peterson parameter in e^+e^- annhilation[a]

Meson	Measured ϵ_P	
	ARGUS	CLEO
D_2^{*0}	0.06 ± 0.03^a (18)	$0.034^{+0.018}_{-0.011} \pm 0.005^a$ (16)
D_2^{*0}	0.054 ± 0.027^b (5)	
D_2^{*+}		$0.020^{+0.011}_{-0.006} \pm 0.003$ (22)
D_1^0	0.040 ± 0.010 (5)	$0.015^{+0.004}_{-0.003} \pm 0.001$ (16)
D_1^+		$0.013 \pm 0.005 \pm 0.004$ (22)
D_{s1}^+	$0.06^{+0.02}_{-0.01} \pm 0.02$ (24)	$0.014^{+0.010}_{-0.005} \pm 0.003$ (25)

[a]This measurement used $D_2^{*0} \to D^+\pi^-$.
[b]This measurement used $D_2^{*0} \to D^{*+}\pi^-$.

Table 10 Measurements of cross section × branching fraction in e^+e^- annhilation[a] at 10.6 GeV

Meson and Decay Mode	$\sigma(e^+e^- \to D^{**}X) \cdot \mathcal{B}(D^{**})$ (pb)	
	ARGUS	CLEO
$D_2^{*0} \to D^+\pi^-$	$68 \pm 21 \pm 28$ (18)	$21.4 \pm 3.4 \pm 4.2$ (16)
$D_2^{*0} \to D^{*+}\pi^-$	$19 \pm 4 \pm 6^a$ (5)	$9.5 \pm 2.4 \pm 1.8$ (16)
$D_2^{*+} \to D^0\pi^+$		$21.9 \pm 7.7 \pm 2.3$ (22)
$D_2^{*+} \to D^{*0}\pi^+$		$11.5 \pm 5.1 \pm 1.4$ (22)
$D_1^0 \to D^{*+}\pi^-$	$32 \pm 4 \pm 9^a$ (5)	$28.5 \pm 2.3 \pm 3.6$ (16)
$D_1^+ \to D^{*0}\pi^+$		$26.4 \pm 7.1 \pm 2.8$ (22)
$D_{s1}^+ \to D^{*+}K^0$	$26 \pm 8 \pm 4$ (27)	$5.8 \pm 1.0 \pm 0.9$ (25)
$D_{s1}^+ \to D^{*0}K^+$	$18 \pm 4 \pm 3$ (27)	$6.5 \pm 1.1 \pm 1.0$ (25)

[a]These values have been corrected for the new D^{*+} branching fraction measurements.

that cannot all be traced to the disagreement over the fragmentation because such a large fraction of the spectrum is at high x. Note that there has been some confusion in the literature concerning the factor of two between the rates for $D_{s1}^+ \to D^{*+}K_S^0$ and $D_{s1}^+ \to D^{*+}K^0$ (see 24 and 25).

The systematic uncertainties are smaller for ratios of production cross sections. We define production ratio $J_A(A \to BC)/J_B$ as the ratio of production cross sections for states A and B times the branching fraction for $A \to BC$. This ratio is usually measured for some x cut applied to both A and B. In this case, no extrapolation to $x = 0$ is necessary, and some of the efficiency and branching fraction uncertainties cancel. Even in terms of these production ratios, the CLEO II measurements are consistently lower than the earlier measurements by CLEO and ARGUS. Table 11 lists some of these measurements, all performed with $x \geq 0.6$.

Table 11 Measurements of production ratios in e^+e^- annhilation (with a cut of $x \geq 0.6$)

Production ratio	Measured values (%)		
	ARGUS	CLEO 1.5	CLEO II
$D_2^{*0} \to D^+\pi^-/D^+$	$11 \pm 4 \pm 5$ (18)	$10 \pm 2^{+2}_{-1}$ (20)	$4.7 \pm 0.7 \pm 0.7$ (16)
$D_2^{*0} \to D^{*+}\pi^-/D^{*+}$		$3.6 \pm 1.0^{+0.4}_{-0.8}$ (20)	$2.1 \pm 0.5 \pm 0.4$ (16)
$D_1^0 \to D^{*+}\pi^-/D^{*+}$		$8.9 \pm 1.1 \pm 0.5$ (20)	$6.8 \pm 0.6 \pm 0.9$ (16)
$D_{s1}^+ \to D^{*+}K^0/D^{*+}$		2.6 ± 0.7 (20)	1.6 ± 0.3 (25)
$D_{s1}^+ \to D^{*0}K^+/D^{*0}$			2.3 ± 0.5 (25)

In one photoproduction experiment at Fermilab, E691, Anjos et al (17) also measured two production ratios. For $D_2^{*0} \rightarrow D^+\pi^-$ and for $D_1^0 \rightarrow D^{*+}\pi^-$ these authors measured ratios of $7 \pm 2 \pm 2\%$ and $13^{+3}_{-2} \pm 2\%$, respectively. No explicit x cut is stated for these measurements. Thus, although the charm production mechanisms may be quite different in e^+e^- annihilation and photoproduction, the fragmentation that determines the production ratio may be very similar.

5. COMPARISON OF EXPERIMENTAL RESULTS AND THEORETICAL PREDICTIONS

As stated above, the only measurements of excited charmed mesons are of the P-wave states. In this section, we first discuss the isospin splittings between charged and neutral states and the splittings within the $j = 3/2$ doublets. We then compare the experimental data with the quark model predictions of Godfrey & Kokoski (7) and the HQS predictions of Eichten et al (referred to as EHQ) (8).

The isospin splitting between the masses of the neutral and the charged D^{**}s is expected to be approximately equal to the D^{*+}-D^{*0} mass splitting (32). The measured mass difference between the D^{*+} and D^{*0} is ~3 MeV. As seen from Tables 5 and 6, the observed isospin splitting for the $j = 3/2$ D^{**} states is consistent with this value.

The mass difference between the two members of each $j = 3/2$ doublet (the $1^+_{3/2}$ and 2^+ states) is independent of the flavor of the light quark, within measurement uncertainties. The average splitting in the D system, designated $\Delta M_D(3/2^+)$, is ~35 MeV. [In fact, the same 35 MeV splitting is seen in the excited charmed baryon doublet reported by CLEO (33).] The corresponding splitting for the K meson system is $\Delta M_K(3/2^+)$ ~160 MeV; the ratio of the splittings is $R_{DK}(3/2^+) = 0.22$.

If HQS with $1/m_Q$ corrections is applicable to both the D and K systems, this ratio should be equal to the ratio of the masses of strange and charm quarks, i.e. $R_{sc} = m_s/m_c$. The ratio of splittings for the ground state doublets (the pseudoscalars and vectors), $R_{DK}(1/2^-)$, should also be equal to R_{sc}. Using the measured masses of the K, $K^*(892)$, D, and D^* mesons yields a value of $R_{DK}(1/2^-) = 0.35$ (1). The difference between the two ratios, $R_{DK}(3/2^+) = 0.22$ and $R_{DK}(1/2^-) = 0.35$, might be an indication that the strange quark is too light for HQS to be applicable to the K system.

5.1 *Heavy-Quark Symmetry*

Eichten et al (EHQ) (8) assume that the splitting within the $j = 3/2$ doublet is inversely proportional to the heavy-quark mass. Furthermore, they assume that the excitation energy above the ground state in the HQS limit depends

only on the radial and orbital quantum numbers of the light quark. These assumptions, together with experimental data on P-wave K and D mesons, are used to predict the masses of other P-wave $j = 3/2$ mesons, i.e. the D_s^{**+}s, B^{**}s, and B_s^{**}s. Comparison with the observed masses should provide a test of these assumptions. If the assumptions are at least approximately valid, the uncertainty in the predictions of EHQ can be estimated using the data. However, because no B^{**} or B_s^{**} has been clearly observed as of yet, the only data that can be used to test these predictions are the masses of the D_s^{**+}s (D_{s1}^{+} and D_{s2}^{*+}). The predicted masses for these states are ~10 MeV lower than the observed masses. However, considering the uncertainties in the mass measurements (their input data have errors ranging from 2 to 10 MeV), the data do not contradict the theoretical assumptions.

Since the prediction of the mass splitting of the $j = 3/2$ doublet in the B meson system does not depend on the K meson masses, it should be accurate. However, the prediction of the central mass value of the doublet is based on both the D and K meson masses. The predictions of masses for states of higher orbital excitations (e.g. $L = 2$) are based on the assumptions discussed above and the measured K meson masses only, since no charm data are available. Thus the accuracy of the predictions depends on the validity of the HQS treatment of the K mesons.

The decay properties of the D_1 and for both members of the $j = 3/2$ D_s^{**+}, B^{**}, and B_s^{**} doublets, were calculated using a transition strength derived from the observed width of the D_2^*; $1/m_Q$ corrections to HQS were ignored. The widths predicted for the $D_1^0(2420)$ and for the $D_{s2}^{*+}(2573)$ are in agreement with the measured values. The width predicted for the $D_{s1}(2536)^+$ is within the current experimental limit. The calculated ratio for the D_2^* decay rates to $D\pi$ and $D^*\pi$ is ~2 and is consistent with the measured value. However, both the predicted and the measured values have large uncertainties. Table 12 summarizes some of these comparisons.

5.2 *Quark Model*

In this section, we compare the experimental results with the quark model predictions of Godfrey & Kokoski (7), who used a model with one set of parameters to calculate the masses of all mesons, from pions to B mesons (34). The masses of the S-wave charmed meson are overestimated by 10–30 MeV, an indication of the size of the uncertainty in these mass predictions. The mass predicted for the 2^+ D^{**} is 40 MeV higher than that of the D_2^*, the observed state with which it is identified. The two $J = 1$ states are within ~10 MeV of each other. The lower-mass state, which Godfrey & Kokoski termed Q_{cL}, is identified with the observed D_1 because of its narrow width. The predicted mass is again ~40 MeV higher than the measured mass. The predicted masses

Table 12 Comparison of the measured masses and widths (in MeV) with recent theoretical predictions[a]

Quantity	Experiment	G & K (7) PSE	G & K (7) FTB	EHQ (8)
D_2^* mass	2459 ± 2	2500		2459 (input)
D_1 mass	2423 ± 2	2460		2424 (input)
D_{s2}^{*+} mass	2573 ± 2	2590		2561
D_{s1}^{+} mass	2535.3 ± 0.5	2561		2526
D_2^* width	24 ± 4	63	37	28[a]
D_1 width	19 ± 4	26	38	18
D_{s2}^{*+} width	16 ± 6	21	16	11
D_{s1}^{+} width	<2.3	0.4	1.9	<1

[a]This total width was partially constrained to agree with data.

of the charmed strange 2^+ and $1^+_{3/2}$ states are ~20 MeV higher than those of the D_{s2}^{*+} and D_{s1}^{+}, the observed states with which they are identified. Note that the calculated splitting between the 2^+ and $1^+_{3/2}$ states agrees much better with the observed value than the calculated average mass does with the corresponding observed value.

Godfrey & Kokoski used two different models for the decay, a pseudoscalar emission (PSE) model and a flux tube–breaking (FTB) model (7), to calculate the partial widths of the various states. They took the difference between the two sets of results as a measure of the uncertainty in the predictions. The calculated width of the $J = 2$ D^{**} is two or three times larger than the value measured for the D_2^*. In light of the uncertainties in the measurements and in the calculation, these predictions cannot be considered inconsistent with the measured values.

The predicted ratio for the decay rates of the D_2^* to $D\pi$ and $D^*\pi$ is again ~2, a result consistent with the measured value. The observed width of the $D_{s2}^{*+}(2573)$ is also in agreement with the quark model prediction.

For the higher-mass $J = 1$ state, which these authors term $\mathcal{Q}_{cH}$, there is a neglible contribution to the decay from the D-wave amplitude. In both decay models, the width resulting from the S-wave amplitude is much too large to be consistent with the ~20 MeV width measured for the D_1.

For the $\mathcal{Q}_{cL}$, the S-wave amplitude is strongly suppressed. However, because the S-wave phase space is so large, the D- and S-wave partial widths can be comparable. The contributions from these two amplitudes, especially the S-wave, vary greatly between the two models. As a result, the total width as

well as the fraction of decays proceeding via a D wave depends strongly on the model. The predicted total widths from the PSE and FTB models are 26 and 38 MeV, respectively. (These partial widths and those in Table 12 are taken directly from Godfrey & Kokoski's paper, using their predictions for masses. Using the measured masses will change some of the predictions by up to 20%.) The fraction of D-wave decays varies from 30% in the FTB model to 80% in the PSE model. The observed helicity angle distributions indicate that the decay is more likely predominantly a D-wave decay. On the basis of the calculated value of the singlet-triplet mixing angle, the predictions of the PSE model agree better with the measured width and helicity angle. On the other hand, the observed width of the $J = 2$ state (D_2^*) favors the FTB model calculations. Thus, the experimental data do not show a clear preference for one model over the other.

The decay properties of the $J = 1$ states are also sensitive to the mixing angle, and were it not for the large uncertainty resulting from the modeling of the decay, the experimental data could be used to determine, or at least constrain, the mixing angle.

The observed state, the $D_{s1}^+(2536)$, is identified as the lower-mass strange $J = 1$ state on the basis of its narrow width. The measured 90% c.l. upper limit on the width of the D_{s1}^+ is consistent with the predictions of both models.

Finally, we note that the most accurate mass measurement for any P-wave meson (charmed, strange, or flavorless) to date is that of the $D_{s1}^+(2536)$. If theoretical calculations can reproduce this mass, predictions of unobserved states based on these calculations will be more reliable. The relatively tight upper limit on the width of this mass should also provide a good means to constrain parameters used to describe decays.

6. FUTURE MEASUREMENTS

6.1 *Future Measurements of Known Mesons*

The statistical uncertainties in the number of events in a particular decay mode for the observed states typically range from 20 to 25%. The systematic uncertainties often fall in the same range. Consequently, with the current datasets, the ratios of rates for any two decays is not known to better than ~50% from any one experiment. Averaging several experiments reduces the uncertainty, although common systematic errors (in dealing with background, for example) may occur that are not recognized in the averaging. The statistics and the understanding of the background will have to improve considerably before the data on ratios of decay rates can be used to effectively constrain theoretical models.

Fortunately, such improvements are very likely, at least in terms of raw numbers of events. By 1998, we should have datasets an order of magnitude larger than those currently available, both from fixed-target experiments [e.g. FOCUS at Fermilab, formerly known as E831 (35)] and from CLEO. With the concurrent improvements in experimental apparatus, the outlook for much more precise measurements of decay rates is hopeful. On a longer timescale, large samples of charmed mesons will be recorded at the SLAC and KEK B factories (36–38), while more data will be accumulated at CLEO.

On a shorter timescale, using data currently or soon to be available, more decay modes might be observed. These include $D_2^* \to D^*\rho$ and $D_1 \to D\rho$, which might be seen in the next few years. Eichten et al suggest that these modes represent a significant fraction of the total decay rate of these states (8). Improvements in measurements of angular distributions may also make possible the determination of partial wave strengths and relative phases in the decays of the $1^+_{3/2}$ states.

All in all, over the next several years and through the end of the decade, we should see steady improvements in measurements and experimental understanding of the six $j = 3/2$ states.

6.2 *Other Charmed Mesons Yet to be Observed*

6.2.1 BROAD P-WAVE STATES (0^+, $1^+_{1/2}$) The $j = 1/2$ D^{**} states are expected to be several hundreds of MeV wide (7). The resulting broad enhancements located near the edge of phase space in the $D\pi$ and $D^*\pi$ spectra will remain difficult to observe, as will the 0^+ D^{**} states, which decay to DK. The $1^+_{1/2}$ D_s^{**+} may be low enough in mass so as to be relatively narrow (tens of MeV). If its mass were below D^*K threshold, it would be very narrow and would likely decay to $D_s^+\pi\pi$ or to $D_s^{*+}\pi^0$ (39). Unfortunately, this scenario is unlikely. If the $1^+_{1/2}$ D_s^{**+} mass is more than a few MeV above D^*K threshold (2500 MeV), it is predicted to be quite broad. Godfrey & Kokoski (7) predict, in fact, that its mass should be 10 MeV higher than the $D_{s1}^+(2536)$, i.e. ~2545 MeV. Thus it is uncertain whether these broad P-wave states will ever be observable by current methods.

Alternatively, these broad P-wave states could be observable in the decay of some higher-mass state, for instance, B mesons. The ARGUS and CLEO collaborations have observed the decay $B^- \to D_1^0(2420)\pi^-$ (40, 41). The semileptonic decay, $B^- \to D_1^0(2420)\ell^-\bar{\nu}$, has been observed by the ALEPH group and in other LEP experiments (42, for example). At the B factories, the 0^+ and $1^+_{1/2}$ states may be observable in $B \to D^{**}\ell\nu$ decay, either directly or in interference with the $j = 3/2$ states.

6.2.2 HIGHER EXCITED STATES None of the higher excited states has been observed as of yet. Such states include radial excitations and higher orbital excitations (i.e. 2S, 3D states). They are expected to be broader than the P-wave states observed to date. Eichten et al, extrapolating from the D-wave K mesons, predict that the $L = 2$, $j = 5/2$ states will have widths of ~60–240 MeV and masses ~400 MeV higher than those of the P-wave states (8). The EHQ prediction for the masses of these states is 2830 MeV for the nonstrange and 2880 MeV for the strange D-wave charmed mesons. The production cross sections, the reconstruction efficiency, and the ability of the experimenters to separate the signal from background are all uncertain. However, they may be easier to find than the broad P-wave states.

We end this section with a final note on the P-wave mesons. A large part of the background in the mass spectra used to study these mesons arises from decays of other excited charmed mesons. As new excited states are observed and their decays become known and as the contributions of other P-wave states are measured more precisely, the background in these spectra will be better understood. This knowledge will make possible more accurate measurements of the P-wave states.

7. CONCLUSIONS

The past decade has seen the discovery of six new charmed mesons, which are now quite well established. Higher excited charmed mesons, and perhaps some of the broad P-wave states, are likely to be observed in the next several years. We also expect improvements in the measurements of the properties of all charmed mesons. Such new observations and measurements should provide more stringent tests of the quark models and of the HQS calculations. They will also improve the accuracy of the predictions by enabling better determination of the free parameters in the calculations. Thus we expect continuing interest and considerable progress in charmed meson spectroscopy for the foreseeable future.

ACKNOWLEDGMENTS

We wish to thank Chris Quigg, Joel Butler, and Rob Kutschke for helpful discussions. This work was supported in part by the US Department of Energy Contract No. DE-AC02-76CH03000 and by the National Science Foundation and Vanderbilt University.

Literature Cited

1. Montanet L, et al. Particle Data Group. *Phys. Rev. D* 50:1173 (1994)
2. Abreu P, et al. DELPHI Collaboration. *Phys. Lett. B* 345:598 (1995)
3. Goldhaber G, et al. Mark I Collaboration. *Phys. Rev. Lett.* 37:255 (1976)
4. Albrecht H, et al. ARGUS Collaboration. *Phys. Rev. Lett.* 56:549 (1986)
5. Albrecht H, et al. ARGUS Collaboration. *Phys. Lett. B* 232:398 (1989)
6. Rosner JL. *Comments Nucl. Part. Phys.* 16:109 (1986)
7. Godfrey S, Kokoski R. *Phys. Rev. D* 43:1679 (1991)
8. Eichten EJ, Hill CT, Quigg C. *Phys. Rev. Lett.* 71:4116 (1993); Eichten EJ, Hill CT, Quigg C. *FERMILAB-CONF-94/188-T* (1994)
9. De Rújula A, Georgi H, Glashow SL. *Phys. Rev. Lett.* 37:785 (1976)
10. Schnitzer HJ. *Phys. Rev. D* 18:3482 (1978)
11. Pignon D, Piketty CA. *Phys. Lett. B* 81:334 (1979)
12. Isgur N, Wise MB. *Phys. Lett. B* 232:113 (1989)
13. Grinstein B. *Annu. Rev. Nucl. Part. Sci.* 42:101 (1992)
14. Neubert M. *Phys. Rep.* 245:259 (1994)
15. Ming-Lu, Wise MB, Isgur N. *Phys. Rev. D* 45:1553 (1994)
16. Avery P, et al. CLEO Collaboration. *Phys. Lett. B* 331:236 (1994)
17. Anjos JC, et al. Fermilab E691. *Phys. Rev. Lett.* 62:1717 (1989)
18. Albrecht H, et al. ARGUS Collaboration. *Phys. Lett. B* 221:422 (1989)
19. Frabetti PL, et al. Fermilab E687. *Phys. Rev. Lett.* 72:324 (1994)
20. Avery P, et al. CLEO Collaboration. *Phys. Rev. D* 41:774 (1990)
21. Albrecht H, et al. ARGUS Collaboration. *Phys. Lett. B* 231:208 (1989)
22. Bergfeld T, et al. CLEO Collaboration. *Phys. Lett.* 340:190 (1994)
23. Kubota Y, et al. CLEO Collaboration. *Phys. Rev. Lett.* 72:1972 (1994)
24. Albrecht H, et al. ARGUS Collaboration. *Phys. Lett. B* 230:162 (1989)
25. Alexander JP, et al. CLEO Collaboration. *Phys. Lett. B* 303:377 (1993)
26. Aguilar-Benitez M, et al. Particle Data Group. *Phys. Lett. B* 170:1 (1986)
27. Albrecht H, et al. ARGUS Collaboration. *Phys. Lett. B* 297:425 (1992)
28. Asratyan AE, et al. BEBC Collaboration. *Z. Phys.* C61:563 (1994)
29. Asratyan AE, et al. *Z. Phys.* C40:483 (1988)
30. Asratyan AE, et al. *Phys. Lett. B* 257:525 (1991)
31. Peterson C, et al. *Phys. Rev. D* 27:105 (1983)
32. Godfrey S, Isgur N. *Phys. Rev. D* 34:899 (1986)
33. Edwards KW, et al. CLEO Collaboration. *Phys. Rev. Lett.* 74:3331 (1995)
34. Godfrey S, Isgur N. *Phys. Rev. D* 32:189 (1985)
35. Bianco S, et al. Wideband Beam Photon Collaboration. *Fermilab Proposal #831* (1992)
36. Hitlin D, ed. *SLAC Rep. #353*, SLAC, Stanford, CA (1989)
37. BABAR Collaboration. Letter of Intent, *SLAC Rep. #433*, SLAC, Stanford, CA (1994)
38. Cheng MT, et al. BELLE Collaboration. *KEK Letter of Intent 94-2* (1994)
39. Cho P, Trivedi SP. *Phys. Rev. D* 50:381 (1994)
40. Albrecht H, et al. ARGUS Collaboration. *Phys. Lett. B* 335:526 (1994)
41. Alam MS, et al. CLEO Collaboration. *Phys. Rev. D* 50:43 (1994)
42. Buskulic D, et al. ALEPH Collaboration. *Phys. Lett. B* 345:103 (1995)